Investigation of the Effect of Impulse Voltage to Flashover by Using Water Jet

Harun Gülan, Muhsin Tunay Gencoglu, Mehmet Cebeci

Abstract—The main function of the insulators used in high voltage (HV) transmission lines is to insulate the energized conductor from the pole and hence from the ground. However, when the insulators fail to perform this insulation function due to various effects, failures occur. The deterioration of the insulation results either from breakdown or surface flashover. The surface flashover is caused by the layer of pollution that forms conductivity on the surface of the insulator, such as salt, carbonaceous compounds, rain, moisture, fog, dew, industrial pollution and desert dust. The source of the majority of failures and interruptions in HV lines is surface flashover. This threatens the continuity of supply and causes significant economic losses. Pollution flashover in HV insulators is still a serious problem that has not been fully resolved. In this study, a water jet test system has been established in order to investigate the behavior of insulators under dirty conditions and to determine their flashover performance. Flashover behavior of the insulators is examined by applying impulse voltages in the test system. This study aims to investigate the insulator behaviour under high impulse voltages. For this purpose, a water jet test system was installed and experimental results were obtained over a real system and analyzed. By using the water jet test system instead of the actual insulator, the damage to the insulator as a result of the flashover that would occur under impulse voltage was prevented. The results of the test system performed an important role in determining the insulator behavior and provided predictability.

Keywords—Insulator, pollution flashover, high impulse voltage, water jet model.

I. Introduction

THERE are natural and unnatural effects in the insulators that affect the flashover. While environmental pollution, climatic conditions and lightning are the natural factors among these effects; industrial pollution, operating conditions and situations such as corona are unnatural factors. Pollution has been proven to have an effect to reduce the performance of the insulator and cause occasional breakdowns by increasing the conductivity on the insulator surface [1]-[4]. When the insulators are dry, a capacitive leakage current is passed through them in very small values and the voltage distribution can be simply defined by the electrostatic field. Leakage currents begin to flow through the polluted surface, which becomes conductive as a result of the pollution layer getting wet by factors such as rain, fog, dew, moisture etc. These leakage currents cause energy loss on the surface. In

Muhsin Tunay Gencoglu and Mehmet Cebeci are with Firat University, Faculty of Engineering, Department of Electrical and Electronics Engineering, Elazig, Turkey (e-mail: mtgencoglu@firat.edu.tr, mcebeci@firat.edu.tr)

Harun Gülan is with Tunceli University, Faculty of Engineering, Department of Electrical and Electronics Engineering, Tunceli, Turkey (e-mail: hgulan@tunceli.edu.tr)

particular, the polluted areas in the narrower areas of the insulator dry out by heating up more forming the parts called "dry band". As a result, the voltage distribution that was primarily homogeneous across the surface deteriorates. Pre-discharges occur when the voltage drop in dry band zones exceeds the puncture resistance of air. Pre-discharges often go out; but in some circumstances, a flashover occurs as a result of the short circuit occurring across the surface. The arc with high current value that occurred as a result of the flashover may cause damage to the insulators, power failure in the energy transmission lines, and even breaking of the power transmission line by melting.

The mathematical modelling of the pollution flashover in insulators started with Obenaus [5] and was developed by other researchers under static and dynamic AC/DC voltages under various conditions. In Fig. 1, it initially had a homogeneous layer of pollution, and then an ideal model of the arc on a flat surface where dry band formation took place. Many researchers used this model with different approaches and achieved the same results [6]-[15]. The assumptions are as follows:

1- Arc length equals dry band length (L_a).
2- Pollution resistance R is a function of the part where only the arc in the surface layer does not occur. That is, R = $R(L_a)$ and $(\partial R/\partial L_a) < 0$.
3- Assuming that the study was carried out in a very short time period, the heating of the layer and the humidity change were neglected.
4- The effect of irregular current density distribution on the arc ends was neglected.

The applied voltage is divided between the layer and the arc according to $V = V_1 + V_a$. Since $V_a = A \cdot I^{-n}$ is defined experimentally,

$$V = I \cdot R(L_a) + A \cdot I^{-n} \qquad (1)$$

happens. Here, the A and n values are the arc constants which vary depending on the ambient conditions where the arc occurs.

$$R(L_a) = R_C (L - L_a) \qquad (2)$$

is given as. If this relation is replaced in (1),

$$V = I \cdot R_C (L - L_a) + A \cdot I^{-n} \qquad (3)$$

is obtained. $R_c = \rho/b$, with the resistivity of the surface layer ρ

World Academy of Science, Engineering and Technology
International Journal of Energy and Power Engineering
Vol:13, No:7, 2019
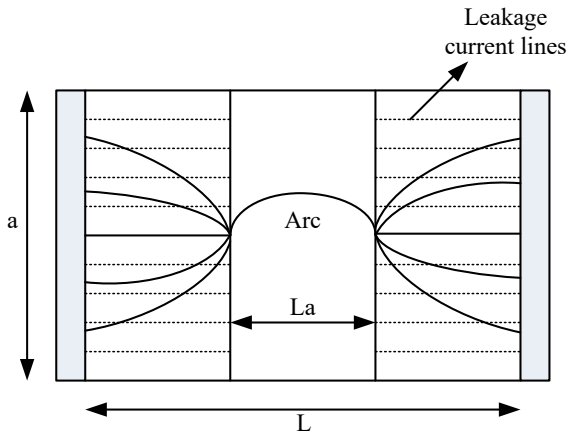
and the width of the pollution layer b.

Fig. 1 Ideal arc model

The function given by (3) is shown graphically in Fig. 2. In the figure, V_a is the voltage falling on the arc at L_a length; V_1 is the voltage falling on the layer at $(L-L_a)$ length; V_m is the required minimum voltage for the continuity of the arc at L_a length and V is the flashover voltage.

If the applied voltage falls below the V_m value, the arc goes out. The I_m current, which realizes such a condition for this minimum voltage, can be found by deriving the derivative V according to I and equalizing to zero.

$$\frac{dV}{dI} = 0 \qquad (4)$$

$$I_m = \left[\frac{A \cdot n \cdot L_a}{R_C (L - L_a)} \right]^{\frac{1}{1+n}} \qquad (5)$$

When we write this I_m value in (3),

$$V_m = (1+n)(A \cdot L_a)^{\frac{1}{n+1}} \left[\frac{R_C (L - L_a)}{n} \right]^{\frac{n}{1+n}} \qquad (6)$$

is obtained [16].

II. High Impulse Voltages

A high impulse voltage is a short-term and single-pole DC HV type. There are four basic sizes that define an impulse voltage. These are: T_1 front time, T_2 half time value, $\hat{V}$ peak voltage value and voltage pole. In addition, the change of voltage over time, namely, the wave form is also important. The type of an impulse voltage shown in Fig. 3 is determined by the peak value, front time, tail (half time value) [17].

A standard type impulse voltage quickly rises to a $\hat{V}$ peak value without a non-standard oscillation and then lowers to zero more slowly. If an intentional or unintentional breakdown

occurs in the high-voltage circuit during the impulse voltage, a sudden drop occurs in the front, peak or tail of the impulse voltage. This type of voltage is called a chopped impulse voltage [18].
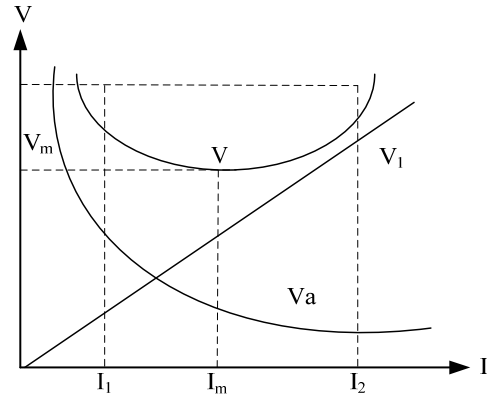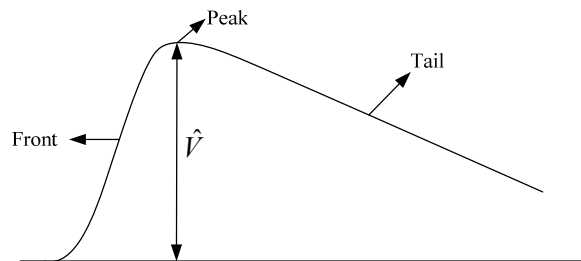

Fig. 2 Voltage curves of the ideal model

Fig. 3 High impulse voltage waveform

A. High Impulse Voltage Types

There are three types of high impulse voltage types that often cause breakdowns in electrical transmission and distribution systems. These are lightning impulse, switching impulse and chopped impulse voltages.

1. Lightning Impulse Voltages

It is a high impulse voltage type in which the overvoltage caused by lightning in nature is in the range of 1 μs. The amplitudes of the impulses are approximately 1000 kV and above. In addition, each lightning impulse causes moving impulse currents to be generated in the transmission line at a maximum insulation resistance level and about 100 kA values. The upright rising edge and the perpendicular edge of the moving waves generate overvoltage on the insulations of power transformers and other high-voltage devices and causes flashovers by sudden breakdown of the insulation at very HV levels. Multiplying the time between 30% and 90% of the peak value of the impulse voltage by 1.67 gives the T_1 front time. The time between the starting point of the impulse voltage and the point where it drops to the 50% of the peak value gives the T_2 half value time [18].

2. Switching Impulse Voltages

It is a high impulse voltage type which occurs in the on-off events of electromechanical devices and where the front time of the internal overvoltage is in the range of 200 μs. The

World Academy of Science, Engineering and Technology
International Journal of Energy and Power Engineering
Vol:13, No:7, 2019

amplitude of such pulses is always related to the application voltage, and the form of the impulse depends on the impedance of the system and switching condition. The voltage rise is slower compared to the lightning impulse voltage type. However, as opposed to the common belief, this waveform can be much more dangerous for insulation systems. Multiplying the time between 30% and 90% of the peak value of the impulse voltage by 1.67 can determine the peak value time of T_p. The time between the starting point of the impulse voltage and the point where the peak value drops to 50% is accepted as the T_2 half value time [18]-[20].

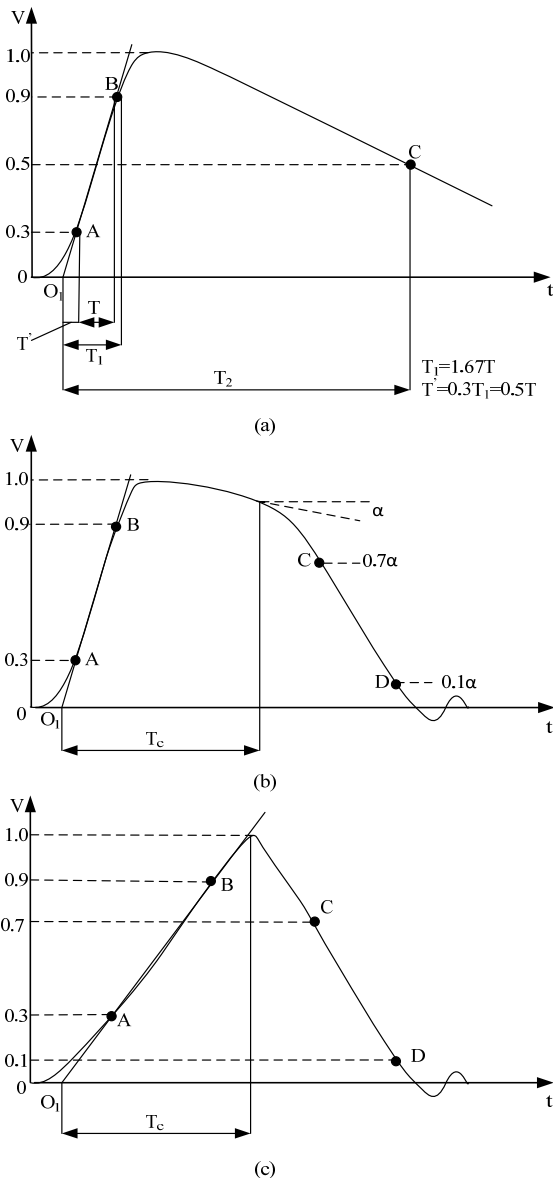### 3. Chopped Impulse Voltages

Fig. 4 Lightning impulse voltage waveform (LI) (a) Full LI (b) LI Chopped on the tail (c) LI Chopped on the front; T_1: Front time, T_2: Time to Half value, T_c: Time to Chopping, O_1: Virtual origin

The high impulse voltages, which are caused by the standard lightning impulse mark falling to zero at the front or the tail of the mark before it can complete itself, is called a chopped impulse voltage (Fig. 4).

In practice, impulse HVs are created with the use of generators for artificial production of similar lightning voltages (lightning impulse), which are formed in the nature and can be explained as a load discharge, and the impulses (switching impulses) generated during switching and short-circuit in a grid in laboratory conditions [21]-[23]. With these generators, the behaviour of HV elements and circuits under high impulse voltage is examined and verified according to national and/or international standards [24], [25].

B. Production of High Impulse Voltages

High impulse voltages are usually achieved by charging the parallel connected capacitors with a special circuit (Marx Generator) from a direct voltage source, and then connecting the same capacitors in series and discharging them into a circuit connected to the test object [24], [26]-[30].

1. Single-Stage Impulse Generators

Fig. 5 shows the circuit of two types of single-stage impulse generators. C_1 value shows the amplitude of the impulse voltage that is pre-charged in the initial state. R_1, R_2 resistances and C_2 capacitor are the circuit elements that perform a very active role in determining the lightning waveform. R_1 resistance damps the circuit and controls the front time T_1. R_2 resistance discharges the capacitors in the circuit and controls the half value time T_2. In a standard circuit, C_2 capacitor acts as a load and varies according to the capacity value of the connected test object.
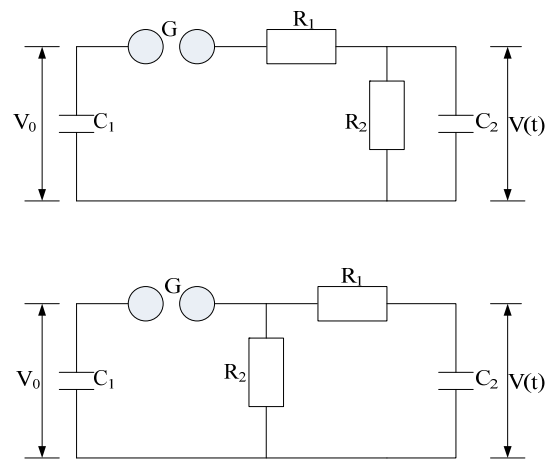

Fig. 5 Single-stage impulse voltage generator equivalent circuit

2. Multistage Impulse Generators

The structure shown in Fig. 6, known as the Marx generator, is used when very HVs are required (Fig. 6). In principle, it consists of single-stage impulse generators connected one after the other. The only difference is the use of R_s resistances which load the capacitors between the stages. Loaded capacitors are discharged into C_2 in series over R_1 resistances with an ignition unit. This operation is realized during T_1. The discharge of the voltage over R_1 and R_2 resistances is realized during T_2 [31], [32].

World Academy of Science, Engineering and Technology
International Journal of Energy and Power Engineering
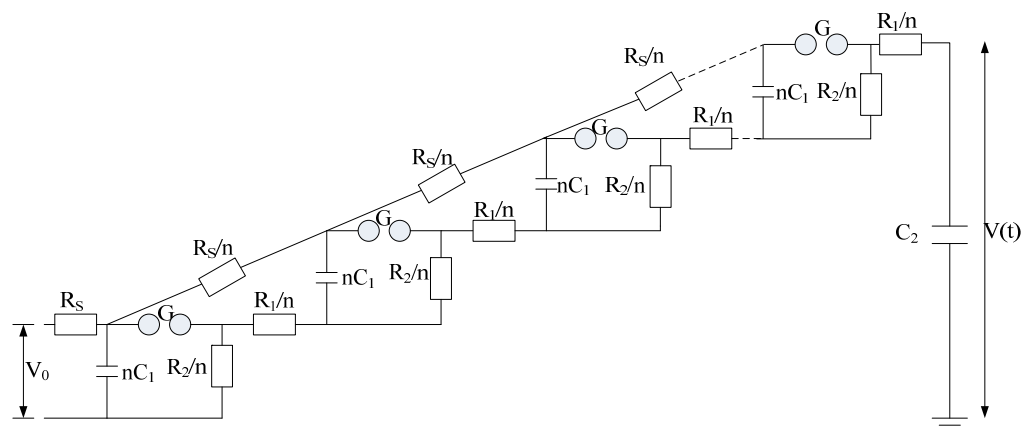Vol:13, No:7, 2019

Fig. 6 Multistage impulse voltage generator equivalent circuit

III. Water Jet Test Set

Various model structures have been used to better understand the physical mechanism of flashover event in HV insulators. The main purpose of these models was to represent the discharged serial pollution zone with a controllable layer whose resistance change is known as much as possible. For this purpose, models coated with various artificial chemical pollutions as well as stagnant and flowing water surfaces were used. The main advantage of using water is that its conductivity can be easily controlled and it can cover the isolated surface homogeneously. Like the other artificial pollutions, the resistance of the water layer undergoes changes under voltage.

The physical model used for flashover tests along the water surface consists mostly of a water channel that has a rectangular cross-section opened to an isolated surface, a low voltage electrode embedded in the water, and a HV electrode is between having a small air gap and the water surface. When sufficient voltage is applied to the HV electrode, the arc may ignite in the air gap. If the voltage applied after the ignition of the arc is gradually increased, it is seen that the arc suddenly spreads and flashes over along the water jet provided that the current and voltage exceed certain values for a given water jet. The steady state before flashover is defined as "critical condition" and the voltage and current values measured under this condition are defined as "flashover voltage" or "flashover current".

The test system, which is used to measure the flashover characteristics caused by the effect of impulse voltage on the water jets at different lengths and conductivity, is given in Fig. 7, and the basic principle scheme is shown in Fig. 8. While measuring the various flashover characteristics, a water jet is prepared with a constant flow and specific conductivity. A salt solution can be mixed into the water in order to change the specific conductivity. Before starting the test, water is circulated through a pump until a good mixture is obtained. The conductivity and water level are continuously controlled during the test to ensure their stability. The water used during the test is collected in a separate water tank.

Test system consists of two main parts as follows:

a. Electrical circuit

b. Water jet mechanism

Fig. 7 200 kV lightning impulse voltage generator and water jet test system

The HV is applied to the water jet circuit using a remote-controlled relay. A two-stage structure is used for the generation of the high impulse voltage. During the tests, the tank level must be kept constant so that speed distribution along the water jet and flow rate does not change. The steel bar with a sharpened tip is used as a high-voltage electrode. For easy and quick adjustment of the jet length, the HV electrode is fixed on a moving isolated system while the grounded jet outlet pipe forming the low voltage electrode is fixed. The jet length is measured by a moving indicator connected to the HV electrode and a fixed ruler mechanism. With this mechanism, the maximum error in jet length measurements is less than 1 mm.

Voltage measurement is carried out with a capacitive voltage divider. In impulse voltages, waveforms of current and voltage are obtained with the help of an oscilloscope.

IV. Test Results

While measuring the various flashover characteristics, first a water jet is prepared whose flow and specific conductivity stays constant. The specific conductivity value can be easily changed by mixing a salt solution into the water. Before starting the test, water was circulated until a good mixture was obtained using a pump and until a constant conductivity was obtained in the conductivity meter. d_0 was obtained by

World Academy of Science, Engineering and Technology
International Journal of Energy and Power Engineering
Vol:13, No:7, 2019

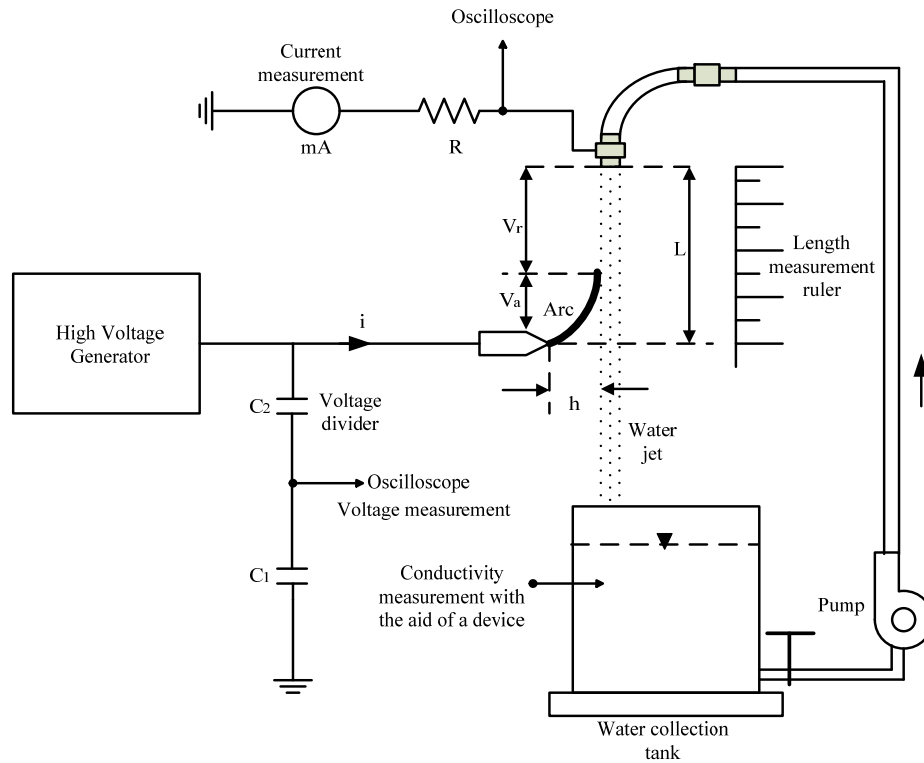measuring the diameter of the water jet on the test system.

Fig. 8 Basic principle scheme of water jet test system

After jet length (L), flow (γ) and first unit resistance (r_0) are set to certain values, the voltage is increased until an arc is formed in a small air gap (h) between the water jet and HV electrode. h air gar represents the dry band forming on the insulator surfaces. If the voltage applied after the ignition of the arc is gradually increased, it is seen that the arc suddenly spreads and flashes over along the water jet provided that the current and voltage exceed certain values for a given water jet.

The sample calculation of r_0 value is as follows:
For σ_0=623 μs/cm conductivity value:

$$s_0 = \pi\left(\frac{d_0}{2}\right)^2 = \pi\left(\frac{4}{2}\right)^2 = 12,56 mm^2 = 0,1256 cm^2 \qquad (7)$$

$$r_0 = \frac{1}{\sigma_0 S_0} = \frac{1}{0,623 \cdot 10^{-3} \cdot 0,1256} = 12779,74 \cong 12,78 k\Omega/cm \qquad (8)$$

is found. During the tests, the flow of the water jet is kept constant at γ = 12.5 cm³/s. This flow rate was chosen to provide a smooth flow through the water column. In the same way, the air gap was kept constant during the tests at h ≈ 2 mm. During the tests, the temperature of the water jet is around 20 °C. (A maximum 1 °C increase was detected due to the post-voltage heating effect applied during the test.)

The data obtained at the time of the flashover during the tests performed according to the pollution values obtained by changing the salt concentration are shown in Table I.

TABLE I
WATER JET FLASHOVER VOLTAGE VALUES WITH DIFFERENT JET LENGTHS AND DIFFERENT INITIAL UNIT RESISTANCE VALUES (KV)

L (cm)	2	3	4	5	6
r_0 = 6,21 kΩ/cm	21,1	25,7	29,5	32,1	39,8
r_0 = 10,56 kΩ/cm	21,6	27,5	33	38,7	46,2
r_0 = 12,78 kΩ/cm	24	29,9	34,1	39,4	47,5

Fig. 9 shows the flashover voltages obtained as a result of the tests conducted by changing the L value between 2-6 cm at three different conductivity values and at each conductivity value. As it is seen, the jumping voltage values increase as the length of the water jet increases. Moreover, the decrease in the initial unit resistance value, i.e. the increase in conductivity, reduced the flashover voltages.

The actual voltage value measured from the oscilloscope was found after the conversion process was carried out with the calibration rate of the designed water jet test system. Also for the current value, the conversion rate of the HV probe applied during the tests was used. Then the waveform data of the voltage and current taken were drawn with the help of MATLAB package program. The time axis of the oscilloscope was subjected to triggering in order to see the changes in waveforms more clearly. For this reason, the time axis in the graphics obtained does not start from zero point. For the same jet length and the same initial unit resistance value, the effect of voltage amplitude value on the flashover situation is shown in Figs. 10-12. As it can be seen, the magnitude of the impulse voltage is directly effective on the system. With the increase in

World Academy of Science, Engineering and Technology
International Journal of Energy and Power Engineering
Vol:13, No:7, 2019

the voltage value, the partial discharges increase and eventually the flashover event occurs.
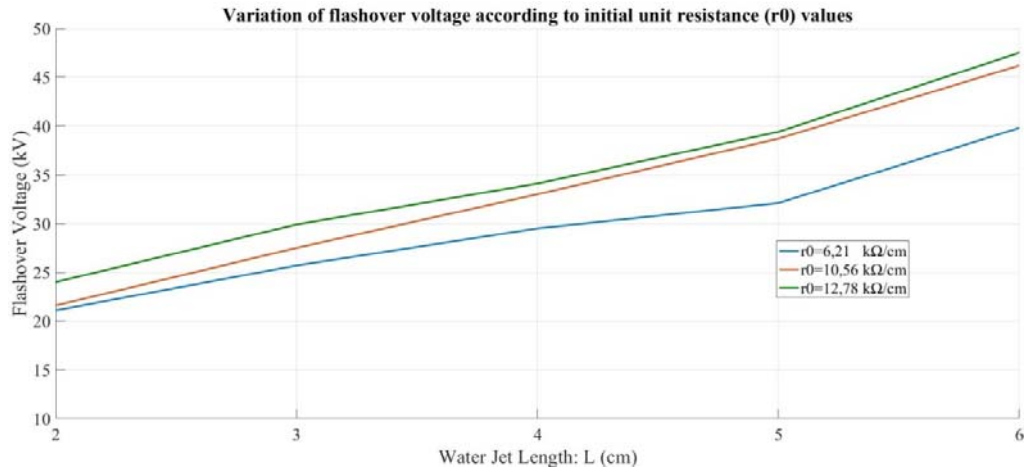
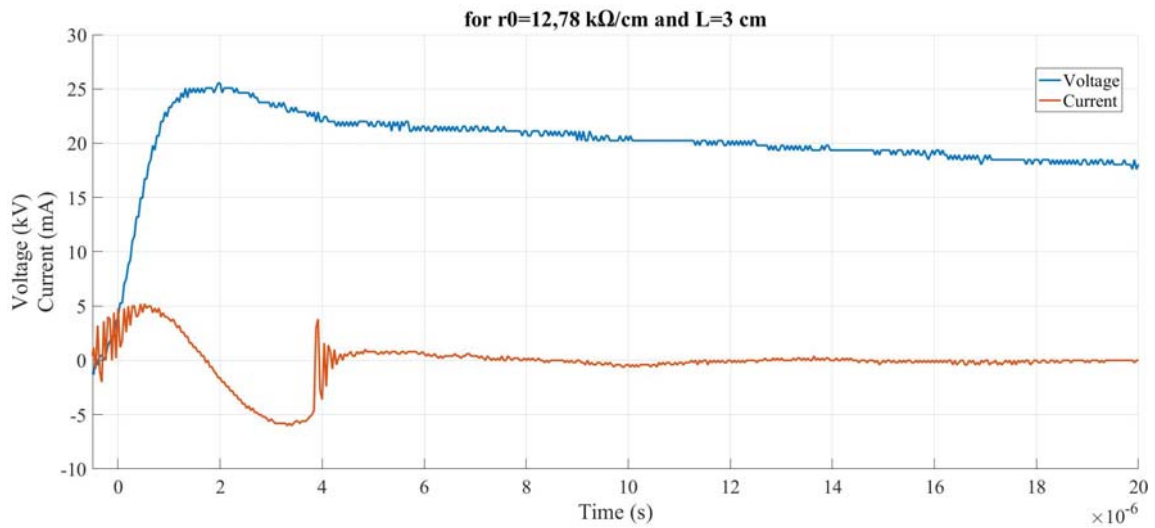Fig. 9 Variation of flashover voltage at different initial unit resistance values

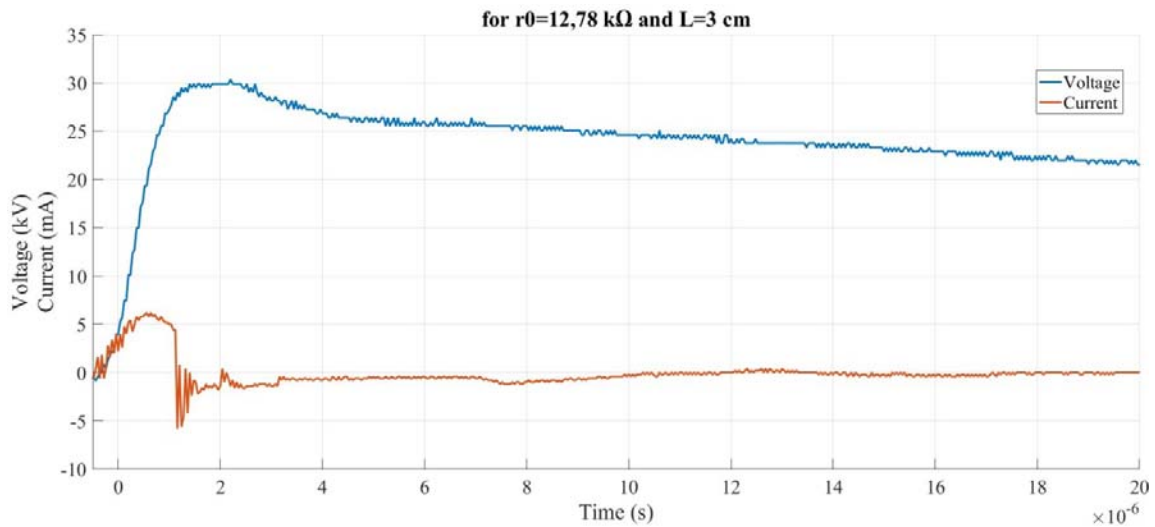Fig. 10 Variation of voltage and current before flashover

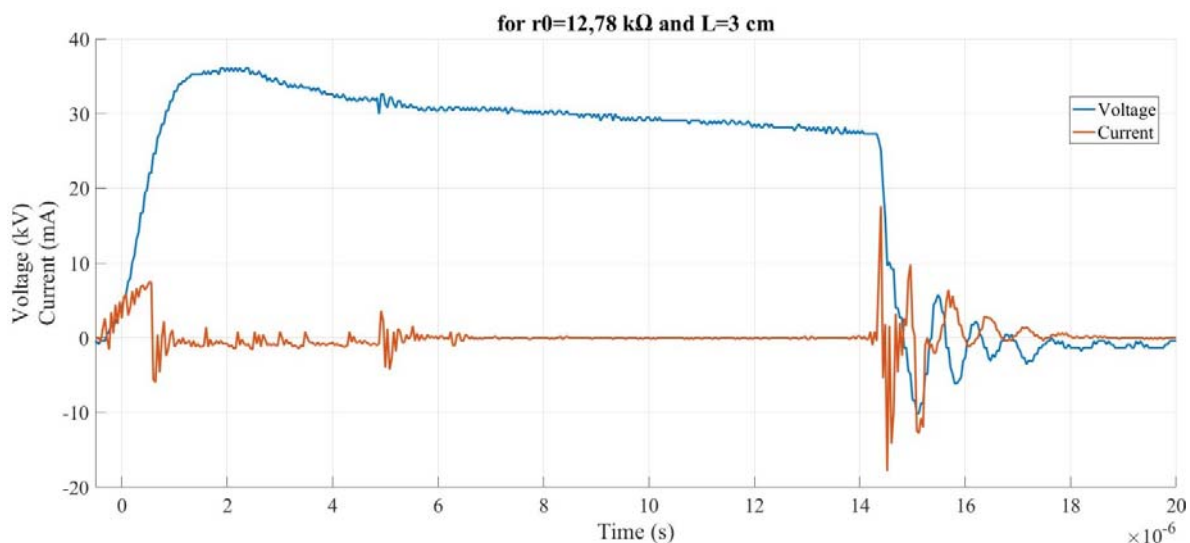Fig. 11 Variation of voltage and current before flashover

World Academy of Science, Engineering and Technology
International Journal of Energy and Power Engineering
Vol:13, No:7, 2019

Fig. 12 Variation of voltage and current at the time of the flashover

V. CONCLUSIONS

The water jet test system designed to predict the pollution flashover behaviour in the insulators yielded very good results. In this way, the flashover mechanism on insulators with various pollution rates was carried out by test studies. As a result of replacing the conductivity of the water with salt solution, flashover characteristics with various pollution values were obtained. In these characteristics, it was seen that the flashover voltage increased in line with the initial unit resistance value. Similarly, the increase in the length of the water jet also increased the flashover voltage. Since the water jet length represents the leakage current path on the insulator in real life, the longer jet length indicates the presence of several interconnected insulators. Although increasing the size of the jet may seem like a good option in increasing the flashover voltage, since this approach will mean increasing the number of insulators, it will not only increase the cost, but also increase the load on the pole and transmission line.

Unlike the AC/DC HV, working with impulse voltages has played an important role in examining the resistance of the insulation material at higher voltage values on the system, even if it is for a very short period of time. Since the impulse voltage was given to the system suddenly (without any increase in voltage level), the behavior of the system was also very fast. This situation caused the partial discharges obtained in the graphics not to be visible. As a result of the impulse voltage applied during the test, either the flashover event occurred or there was no flashover.

REFERENCES

[1] K.J. Lloydand, H.M. Schneider, "Insulation for Power Frequency Voltage. Transmission Line Reference Book (345 kV and Above)", Electric Power Research Institute, Palo Alto, CA, USA, 1982, pp.463-501.
[2] B. Hampton, "Flashover Mechanism of Polluted Insulation", Proc. IEE 111, pp. 985-990, 1964.
[3] F. Obenaus, "Kriechweguberschlag von Isolatoren mit Fremdschichten", Elektrizitatsirtschaft 24 pp. 878-882, 1960.
[4] T.J. Looms, "Insulators for High Voltage", Peter Peregrinus Ltd., London, United Kingdom, 1988.
[5] F. Obenaus, "Contamination flashover and creepage path length", Dtsch. Elektrotechnik 12, pp. 135-136, 1958.
[6] F.A.M. Rizk, "Mathematical models for pollution flashover", Electra 78, pp. 71-103, 1981.
[7] R. Wilkins, "Flashover voltage of high-voltage insulators with uniform surface-pollution films", Proc. IEE 116, pp. 457-465, 1969.
[8] L.L. Alston, S. Zoledziowski, "Growth of discharges on polluted insulation", Proc.IEE 110, pp. 1260-1266, 1963.
[9] S. Gopal, Y.N. Rao, "Flashover phenomena of polluted insulators", Proc. IEE 131, pp.140-143, 1984.
[10] R. Sundararajan, R.S. Gorur, "Dynamic arc modeling of pollution flashover ofinsulators under dc voltage", IEEE Trans. Electr. Insul. 26, pp. 209-218, 1993.
[11] N. Dhahbi-Megriche, A. Beroual, "Flashover dynamic model of polluted insulators under ac voltage", IEEE Trans. Dielectr. Electr. Insul. 7, pp. 283-289, 2000.
[12] N.B. Prakash, M. Parvathavarthini and R. Madavan, "Mathematical Modeling on AC Pollution Flashover Performance of Glass and Composite Insulator", J Electr Eng Technol. 2015; 10(4): pp. 1796-1803.
[13] T. Chihani, A. Mekhaldi, A. Beroual, M. Teguar and D. Madjoudj, "Model for Polluted Insulator Flashover under AC or DC Voltage", IEEE Transactions on Dielectrics and Electrical Insulation Vol. 25, No. 2, pp. 614-622, 2018.
[14] Y. A. Bencherif, A. Mekhaldi and M. Teguar, "Modeling of a high voltage insulator under uniform and non uniform pollution", 2012 Annual Report Conference on Electrical Insulation and Dielectric Phenomena, Montreal, QC, pp. 761-766, 2012.
[15] C. Badachi, P. Dixit, "Prediction of pollution flashover voltages of ceramic string insulators under uniform and non-uniform pollution conditions", Journal of Electrical Systems and Information Technology Volume 3, Issue 2, pp. 270-281, 2016.
[16] Rumeli, A., "Kirli izole yüzeylerde deşarjların yayılımı ve atlama", Elektrik Mühendisliği, 199, s. 419-427, 1973.
[17] Kind, D. and Feser, K., High-Voltage Test Techniques, Vieweg/SBA Publications, New Delhi, 1999.
[18] IEC 60060-1. High-voltage test techniques, Part:1 General definitions and test requirements.
[19] EN 60060-2. High-Voltage Test Techniques, Part:2 Measuring systems, European Standards.
[20] Lucas, J.R., High-Voltage Engineering, Departmant of Electrical

World Academy of Science, Engineering and Technology
International Journal of Energy and Power Engineering
Vol:13, No:7, 2019

Engineering of University of Moratuwa Publications, Sri Lanka, 2001.

[21] A. N. Etobi, N. M. Nor, S. Abdullah, N. Eng Eng and M. Othman,. "Characterizations of a Single Rod Electrode under High Impulse Currents with Different Polarities", 1st International Conference on Electrical Materials and Power Equipment, Xi'an, China, pp. 70-75, 2017.

[22] U. K. Kalla, R. Suthar, K. Sharma, B. Singh and J. Ghotia, "Power Quality Investigation in Ceramic Insulator", IEEE Transactions on Industry Applications, Vol. 54, No. 1, pp. 121-134, 2018.

[23] M. Costea, I. Băran, "The Behavior of High Voltage Insulators during the Up-and-Down Procedure", International Conference on Energy and Environment (CIEM), Bucharest, Romania, pp.11-15, 2017.

[24] Kuffel, E., Zaengl, W.S. and Kuffel J., *High-Voltage Engineering Fundamentals*, Newnes, Toronto, 2000.

[25] Cavallus, N.H., *High Voltage Laboratory Planning*, Haefely, Basel, 1988.

[26] Özkaya, M., *Yüksek Gerilim Tekniği, Cilt 2*, Birsen Yayınevi, İstanbul, 1996.

[27] M.A.B. Sidik, H. Ahmad, I. Ullah, M.N.R Baharom, H.M. Luqman and Z. Zainal, "Small Scale Test Model to Study Impulse Flashover and Attachment Pattern of Protected Building Structures", International Conference on Electrical Engineering and Computer Science (ICECOS), Palembang, Indonesia, pp. 316-320, 2017.

[28] X. Han, J. Li, L. Zhang and Z. Liu, "Partial Discharge Characteristics of Metallic Protrusion in GIS under Different Lightning Impulse Voltage Waveforms Based on UHF Method", IEEE Transactions on Dielectrics and Electrical Insulation Vol. 24, No. 6, pp. 3722-3729, 2017.

[29] M. A. Douar, A. Beroual and X. Souche, "Creeping Discharges Features Propagating in Air at Atmospheric Pressure on Various Materials under Positive Lightning Impulse Voltage–part 1: Noise Suppression Using the Discrete Wavelet Transform Approach", IET Gener. Transm. Distrib., Vol. 12 Iss. 6, pp. 1417-1428, 2018.

[30] Z. Zhang , D. Wei, D. Zhang, J. Zhu and C. Li. "Study on the Lightning Strike Discharge Characteristics of Switchgear Air Gap at Low Air Pressure Condition", IET Gener. Transm. Distrib., Vol. 12 Iss. 9, pp. 2148-2154, 2018.

[31] Naidu, M.S. and Kamaraju, V., *High-Voltage Engineering*, McGraw-Hill, New York, 1995.

[32] J. M. Koutsoubis, J. W. Gray, N. D. Kokkinos and D. N. Kokkinos, "Development and Testing of a 200kA, 10/350μs Lightning Impulse Current Generator Switch Module", IEEE 21st International Conference on Pulsed Power (PPC), Brighton, UK, p 1-4, 2017.